Carbon-enhanced metal-poor stars in dwarf galaxies

Salvadori, Stefania; Skúladóttir, Ása; Tolstoy, Eline

Published in:
Monthly Notices of the Royal Astronomical Society

DOI:
10.1093/mnras/stv1969

Monthly Notices
of the
ROYAL ASTRONOMICAL SOCIETY

MNRAS **454,** 1320–1331 (2015) doi:10.1093/mnras/stv1969

Carbon-enhanced metal-poor stars in dwarf galaxies

Stefania Salvadori,[⋆†] Ása Skúladóttir and Eline Tolstoy

Kapteyn Astronomical Institute, University of Groningen, Landleven 12, NL-9747 AD Groningen, the Netherlands

Accepted 2015 August 21. Received 2015 August 21; in original form 2015 June 9

ABSTRACT

We investigate the frequency and origin of carbon-enhanced metal-poor (CEMP) stars in Local Group dwarf galaxies by means of a statistical, data-calibrated cosmological model for the hierarchical build-up of the Milky Way and its dwarf satellites. The model self-consistently explains the variation with dwarf galaxy luminosity of the observed: (i) frequency and [Fe/H] range of CEMP stars; (ii) metallicity distribution functions; (iii) star formation histories. We show that if primordial faint supernovae dominated the early metal-enrichment, then CEMP-no stars enriched by the first stellar generations should be present in *all* dwarf galaxies, with similar number of stars and CEMP fractions at [Fe/H] < -4. We demonstrate that the probability to observe a star that is carbon-enhanced within a given [Fe/H] range strongly depends on the luminosity of the dwarf galaxy and, on average, it is an order of magnitude lower in 'classical' Sculptor-like dwarf spheroidal (dSph) galaxies ($P \leq 0.02$) than in the least luminous ultra-faint dwarfs ($P \approx 0.1$). In addition, we explain why it may be easier to find CEMP-no stars at [Fe/H] ≈ -2 in classical dSph galaxies than in ultra-faint dwarfs. These are consequences of the dramatic variation in the fraction of stars at [Fe/H] < -3 with galaxy luminosity: $\geq$40 per cent for galaxies with $L < 10^5$ L$_\odot$, and $\leq$0.2 per cent for $L > 10^7$ L$_\odot$. We present model predictions for the low-Fe tail and CEMP fraction of stars in dwarf galaxies, with particular emphasis on the Sculptor dSph, that can be used to shed light on the properties of the first stars.

Key words: stars: abundances – galaxies: dwarf – galaxies: high-redshift – Local Group – cosmology: theory.

1 INTRODUCTION

Understanding the nature of the first stars is one of the key questions of modern cosmology. Despite extensive observational searches, truly pristine stars have so far escaped detection. Currently, the most metal-deficient star known has a total metallicity of $Z \approx 6.9 \times 10^{-7}$ (Caffau et al. 2011). The persistent lack of more metal-poor stars seems to confirm the idea that primordial stars were all more massive than $\approx$1 M$_\odot$ (e.g. McKee & Tan 2008; Hosokawa et al. 2011; Hirano et al. 2014), and that their formation was possibly quenched at early times (e.g. Salvadori, Schneider & Ferrara 2007; Pallottini et al. 2014). However, the chemical signatures of these extinct stellar generations could be retained in the photospheres of ancient (>12 Gyr) low-mass second-generation stars, which formed in pre-enriched environments, $Z > Z_{\rm cr} = 10^{-5\pm1}$ Z$_\odot$, where metals and dust grains dispersed by the first stars enabled efficient gas cooling and fragmentation (e.g. Schneider et al. 2002). These stellar fossils should be observable in the oldest stellar components of our Galaxy and in its ancient dwarf satellites.

High- and medium-resolution spectroscopic studies of Galactic halo stars have revealed the existence of a population of carbon-rich stars (e.g. Beers & Christlieb 2005; Aoki et al. 2007; Lee et al. 2013; Norris et al. 2013; Yong et al. 2013). These objects are usually defined to have carbon-to-iron ratio [C/Fe] > 0.7 (Aoki et al. 2007), and they can be divided into two main populations: carbon-rich stars that exhibit an excess in heavy elements formed by slow (or rapid) neutron capture processes, CEMP-s (CEMP-r) stars, and carbon-rich stars that do not exhibit such an excess, carbon-enhanced metal-poor (CEMP)-no stars. The available data are consistent with the idea that CEMP-s stars belong to binary systems (Lucatello et al. 2005; Starkenburg et al. 2014), and have acquired their carbon-excess from an asymptotic giant branch (AGB) companion (e.g. Bisterzo et al. 2012; Placco et al. 2013; Abate et al. 2015). Thus, the chemical abundances measured in these stars are not representative of the interstellar medium (ISM) out of which they formed. On the other hand, CEMP-no stars are *not* preferentially associated with binary systems (Cohen et al. 2013; Hansen, Andersen & Nordström 2013; Norris et al. 2013; Starkenburg et al. 2014). Hence there is no observational evidence supporting the idea

⋆ E-mail: salvadori@astro.rug.nl
† VENI Fellow.

of mass transfer as the origin of their chemical abundances, which was suggested by some authors (e.g. Suda et al. 2004; Komiya et al. 2007). Furthermore, both their *frequency* and *carbon-excess* increase with decreasing [Fe/H] (e.g. Lucatello et al. 2005; Lee et al. 2013; Norris et al. 2013), and eight out of the nine halo stars discovered at [Fe/H] < -4.5 are CEMP-no stars (Christlieb et al. 2002; Frebel et al. 2005; Norris et al. 2007; Keller et al. 2014; Allende Prieto et al. 2015; Bonifacio et al. 2015; Frebel et al. 2015; Hansen et al. 2015). These findings favour the idea that CEMP-no stars are a peculiar stellar population and that their chemical abundances likely reflect their birth environment.

The unusual chemical compositions of the most iron-poor and carbon-rich stars can be successfully matched by models of *primordial faint supernova (SN)* that experienced mixing and fallback, hence releasing small amounts of iron and large amounts of carbon and other light elements (e.g. Umeda & Nomoto 2003; Iwamoto et al. 2005; Joggerst, Woosley & Heger 2009; Marassi et al. 2014; Tominaga, Iwamoto & Nomoto 2014). Relatively good agreement with observations is also obtained by models of zero- (or very low-) metallicity massive 'spinstars', which experience mixing and mass-loss because of their very high rotational velocities (e.g. Meynet, Ekström & Maeder 2006; Meynet et al. 2010; Maeder, Meynet & Chiappini 2015). Recently, chemical evolution studies have further supported the idea of the link between primordial *faint* SN and CEMP-no stars, showing that the observed fraction of carbon-enhanced to carbon-normal stars at [Fe/H] < -3 is successfully reproduced *if faint SN dominated the early metal-enrichment* (Cooke & Madau 2014; de Bennassuti et al. 2014). Thus, we can work under this simple hypothesis to predict the frequency of pristine carbon-enhanced stars in *ancient* and *metal-poor* dwarf galaxies.

CEMP stars have been found in a significant fraction in the faintest satellites of the Milky Way, the so-called ultra-faint dwarf galaxies, with total luminosities $L \leq 10^5\,L_\odot$ (e.g. Frebel et al. 2010b; Norris et al. 2010; Lai et al. 2011; Gilmore et al. 2013; Frebel, Simon & Kirby 2014). Different groups have proposed these galaxies to be the living relics of the first star-forming minihaloes, which formed in the Milky Way environment prior the end of reionization (e.g. Bovill & Ricotti 2009, 2011; Muñoz et al. 2009; Salvadori & Ferrara 2009, 2012; Salvadori et al. 2014). These theoretical predictions are consistent with recent observations of star formation histories (SFHs) in ultra-faint dwarf galaxies (e.g. Brown et al. 2012, 2014; Dall'Ora et al. 2012; Okamoto et al. 2012). In particular, by interpreting the observed Fe–Luminosity relation and metallicity distribution function (MDF) of dwarf galaxies in a cosmological context, Salvadori & Ferrara (2009) predicted these ancient ultra-faint dwarf galaxies to be the best objects to look for the chemical imprints of the first stellar generations. This picture is supported by the recent discovery of several CEMP-no stars at [Fe/H] < -3 in Segue 1 (Frebel et al. 2014), which is one of the faintest ultra-faint dwarfs.

However, CEMP stars seem to be rare in the more luminous 'classical' dwarf spheroidal (dSph) galaxies, $L > 10^5\,L_\odot$, where measurements are available for larger stellar samples. The deficiency of CEMP(-no) stars is especially mysterious in the Sculptor dSph galaxy. The observed colour–magnitude diagram (CMD) and MDF of Sculptor are consistent with this galaxy being dominated by ancient stars, >10 Gyr old (de Boer et al. 2012). However, no CEMP stars have been found among the 10 carefully studied stars at [Fe/H] < -3 (Frebel, Kirby & Simon 2010a; Tafelmeyer et al. 2010; Starkenburg et al. 2013; Jablonka et al. 2015; Simon et al. 2015). Only recently, the first CEMP-*no* star has been discovered at [Fe/H] ≈ -2 (Skúladóttir et al. 2015). The observed chemical abundance pattern of this star is consistent with the idea that the carbon excess is the result of a *pristine* population of faint SN polluting its birth environment. However, the lack of CEMP-no stars at lower [Fe/H] is not. The important question is, are CEMP stars missing in classical dSph galaxies, or are they hidden?

We argue they may be hidden. To sustain this thesis, in this paper we use a statistical, data-calibrated cosmological model for the formation of the Milky Way and its dwarf satellites, to predict the frequency of CEMP(-no) stars in Sculptor and other Local Group dwarf galaxies. We present a simple, global scenario that self-consistently explains the variation with galaxy luminosity of the observed: (i) carbon-enhanced to carbon-normal star ratios; (ii) metallicity distribution functions; and (iii) star formation histories. We link the properties of Local Group dwarf galaxies with first stellar generations and early galaxy formation processes, and present model predictions aimed at identifying the hidden CEMP-no stars in the classical dSph galaxy Sculptor.

For consistency with previous works (Salvadori & Ferrara 2009, 2012; Salvadori et al. 2014), along with Via Lactea II, Aquarius, and CLUES simulations (e.g. Madau et al. 2008; Wang et al. 2012; Benítez-Llambay et al. 2015), we adopt a Lambda cold dark matter (ΛCDM) cosmology with $\Omega_\mathrm{m} = 0.24$, $\Omega_\Lambda = 1 - \Omega_\mathrm{m} = 0.76$, $\Omega_\mathrm{b} = 0.04$, and $H_0 = 73\,\mathrm{km\,s^{-1}\,Mpc^{-1}}$. Furthermore, in the overall paper we assume the solar abundance values by Asplund et al. (2009).

2 OBSERVATIONS OF CARBON-RICH STARS

Current observations of CEMP stars, [C/Fe] > 0.7, are shown in Fig. 1, where we present a sample of stars from the literature with measured carbon-to-iron ratio, [C/Fe], and iron-abundance, [Fe/H], in both the Galactic halo and nearby dwarf galaxies. Most of these data are based on one-dimensional local thermodynamic equilibrium stellar model analysis.

Measurements for *halo stars* are from Placco et al. (2014), who selected among all available data (see references therein) a sample of 505 stars with [Fe/H] < -2 and [C/Fe] measurements. This sample includes dwarf and giant stars ($0 < \log g < 5$). Placco et al. (2014) corrected [C/Fe] to account for the depletion of surface carbon abundance, which is expected to occur on the upper Red Giant Branch (RGB), $\log g < 2$. The correction depends on several observed quantities: $\log g$, [C/Fe], [Fe/H] and also, to a lesser extent, on [N/Fe]. Hence, we should keep in mind that the corrected values presented in Fig. 1 have intrinsic errors, which are estimated by the authors to be always within the 2σ uncertainties of the [C/Fe] measurements, i.e. ± 0.3 dex.

In more distant dwarf galaxies only the brighter RGB stars are typically observed. Hence, in our selection of dwarf galaxy stars, if the internal mixing was not already accounted for by the authors, we used the online tool by Placco et al. (2014) to self-consistently correct the [C/Fe] measurements. When not available from observations we simply assumed [N/Fe] $= 0.0$, in agreement with Placco et al. (2014). The data shown in Fig. 1 represents the largest sample of [C/Fe] measurements that have been homogeneously corrected to account for internal mixing processes.

From Fig. 1, we can note that stars at [Fe/H] ≤ -4.5 have only been found in the Galactic halo. Moreover, we can see that the frequency of CEMP-no stars among these 'hyper-iron-poor stars' is extremely high: eight out of nine stars at [Fe/H] ≤ -4.5 are CEMP-no stars. These objects have peculiar chemical abundance patterns consistent with the yields predicted for primordial faint

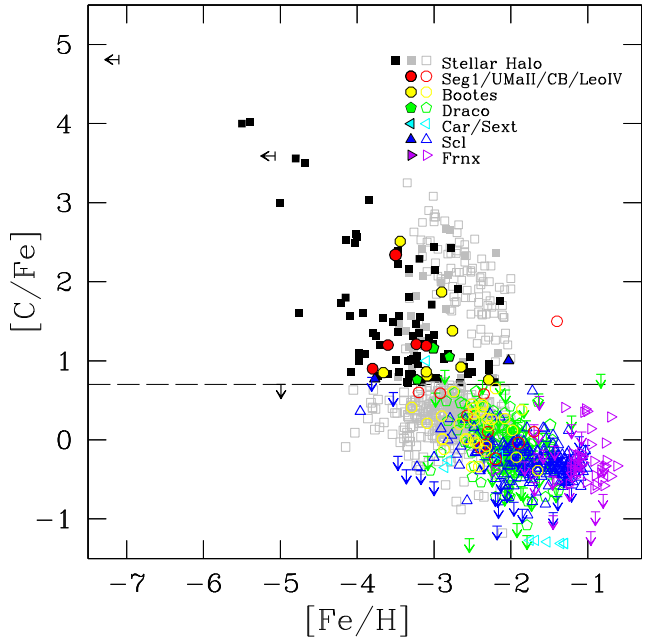

Figure 1. Compilation of stars with measured [C/Fe] and [Fe/H] in the stellar halo (squares), ultra-faint dwarf galaxies (circles, hexagons, pentagons) and classical dSph galaxies (triangles). [C/Fe] measurements are corrected to account for internal mixing processes (see text). CEMP-no stars are shown as filled symbols, upper limits with arrows. Stars with [C/Fe] > 0.7 and open symbols are CEMP-s/r stars. Filled grey squares are CEMP stars with no available measurements of r- or s-process elements. Colours/symbols identify stars in dwarf galaxies with increasing total luminosity: from red to blue (see labels and text). References: *Halo stars:* Placco et al. (2014), Christlieb et al. (2002), Frebel et al. (2005), Norris et al. (2007), Caffau et al. (2011), Keller et al. (2014), Hansen et al. (2015), Bonifacio et al. (2015), Frebel et al. (2015). *Segue 1:* Norris et al. (2010), Frebel et al. (2014). *Ursa Major II* and *Coma Berenice:* Frebel et al. (2010b). *Leo IV:* Simon et al. (2010). *Bootes:* Lai et al. (2011), Norris et al. (2010), Gilmore et al. (2013). *Draco:* Cohen & Huang (2009), Shetrone et al. (2013), Kirby et al. (2015). *Sextans:* Honda et al. (2011). *Carina:* Venn et al. (2012). *Sculptor:* (Frebel et al. 2010a), Tafelmeyer et al. (2010), Starkenburg et al. (2013), Simon et al. (2015), Kirby et al. (2015), Jablonka et al. (2015), Skúladóttir et al. (2015). *Fornax:* (Kirby et al. 2015).

SN (e.g. Iwamoto et al. 2005). However, we also note that these extreme stars are part of a common, global trend, which involves stars in both the Galactic halo and dwarf galaxies. We see that on average [C/Fe] is higher in stars with lower [Fe/H], and it declines with [Fe/H]. The same trend affects the incidence of CEMP-no stars with respect to the overall stellar population. At [Fe/H] ≤ -3.0, the fraction of CEMP-no stars in the Galactic halo, (≈43 per cent; Placco et al. 2014), is consistent with the *overall* fraction of CEMP-no stars in dwarf galaxies, where 24 stars at [Fe/H] ≤ -3 have been observed, and 10 of them are found to be CEMP-no stars. This gives $F_{\rm CEMP}(<-3) \approx 42$ per cent. However, when we consider individual dwarf galaxies, the fractions are highly variable.

The carbon measurements in the least luminous ultra-faint dwarf galaxies, $\log(L/{\rm L}_\odot) < 4.0$ (shown in Fig. 1 with red circles), are from high-resolution spectroscopic studies (see caption for references). Although less than 20 stars have been observed in these four systems, the overall frequency of CEMP-no stars is very high, and at [Fe/H] ≤ -3, five out of six stars are CEMP-no stars, $F_{\rm CEMP}(\leq -3) \approx 83$ per cent. With the only exception of seven stars in Bootes, one of which is a CEMP-no at [Fe/H] $= -3.5$ (Gilmore et al. 2013), only low-resolution spectroscopic studies are available for dwarf galaxies with luminosities between ultra-faint and classical dSph galaxies, e.g. *Bootes*, $\log(L/{\rm L}_\odot) = 4.5 \pm 0.1$, and *Draco*, $\log(L/{\rm L}_\odot) = 5.45 \pm 0.10$. Thus, slow and rapid n-capture elements have not been measured in these stars, preventing us from distinguishing between CEMP-no and CEMP-r/s stars. As discussed in Section 1, however, there is strong observational evidence that CEMP-no stars should be the dominant CEMP population at [Fe/H] < -3 (e.g. Norris et al. 2013). In these dwarf galaxies the fraction of CEMP(-no) stars at [Fe/H] ≤ -3 is high: four out of six stars in Bootes (≈66 per cent), and two out of five stars in Draco (≈40 per cent). The classical dSph galaxies *Carina* and *Sextans*, $\log(L/{\rm L}_\odot) \approx 5.6$, have been followed up at high resolution, but only stars at [Fe/H] ≥ -3 have carbon measurements (see Fig. 1).

In the *Sculptor* dSph galaxy, $\log(L/{\rm L}_\odot) = 6.34 \pm 0.16$, many carbon measurements are available from both low- (Kirby et al. 2015), and high-resolution spectroscopic studies (Frebel et al. 2010a; Tafelmeyer et al. 2010; Starkenburg et al. 2013; Simon et al. 2015; Skúladóttir et al. 2015). In total, 10 stars have been found at [Fe/H] ≤ -3. After correcting for internal mixing, we find that the star Scl_11_1_4296 observed by Simon et al. (2015) at [Fe/H] $= -3.77$ can be possibly identified as a CEMP-no star, [C/Fe] $= 0.77 \pm 0.34$. This was not claimed by the authors, who used the luminosity dependent criteria developed by Aoki et al. (2007) to identify CEMP stars.[1] However, the carbon-excess is small and the errors big, making this classification very uncertain. Thus, the only reliable CEMP-no star discovered in Sculptor, [C/Fe] $= 1.01 \pm 0.1$, has an unusually high iron-abundance, [Fe/H] ≈ -2 (Skúladóttir et al. 2015), which makes this star stand out with respect to the general trend in dwarf galaxies (Fig. 1). No CEMP-no stars have been found in Fornax, $\log(L/{\rm L}_\odot) \approx 7.25 \pm 0.11$, although carbon measurements are only available for stars at [Fe/H] > -2. For other ultra-faint dwarfs (e.g. Segue 2, Willmann, Hercules) or classical dSph galaxies (e.g. LeoT, LeoI, LeoII, Ursa Minor) carbon measurements are not yet available.

In conclusion, while $F_{\rm CEMP}(\leq -3)$ in the Galactic halo is consistent with the *overall* fraction of CEMP-no stars at [Fe/H] ≤ -3 in dwarf galaxies, the individual Milky Way companions show that $F_{\rm CEMP}(\leq -3)$ strongly decreases when the luminosity of the galaxies increases. Does the fraction of CEMP-no stars depend on galaxy luminosity? And why does the only CEMP-no star observed in a more luminous dSph galaxy have an unusually high [Fe/H] ≈ -2? Are these observational findings reconcilable with the idea that the birth environment of CEMP-no stars was polluted by primordial faint SN, and thus consistent with what we see in the Galactic halo?

3 COSMOLOGICAL MERGER-TREE MODEL

We use the data-constrained cosmological code GAMETE (GAlaxy MErger Tree and Evolution; Salvadori et al. 2007, 2014; Salvadori & Ferrara 2009, 2012; de Bennassuti et al. 2014) to link the properties of ancient stars in the Local Group with the early star formation (SF) and metal-enrichment processes. GAMETE describes the formation of the Galaxy and its dwarf satellites in a ΛCDM framework, self-consistently accounting for the key physical processes driving the formation and evolution of high-redshift dwarf galaxies: (i) the transition from *massive*, and hence short-lived Population III (Pop III) stars, to *normal* Population II (Pop II) stars; (ii) the gradual

[1] There are small differences between the Aoki et al. (2007) criteria and the carbon correction by Placco et al. (2014).

quenching of SF in dwarf galaxies with increasing total masses due to the enhanced photodissociating and photoionizing radiation; (iii) the steady metal-enrichment of the Milky Way environment, or *Galactic medium*, due to SN-driven outflows from star-forming haloes.

Our model is a statistical tool that enables us to study the most likely assembly and metal-enrichment histories of Local Group galaxies. The SF and chemical evolution of present-day galaxies is traced across cosmic time by exploiting a sample of merging histories of a Milky Way-size dark matter halo ($M_{\rm MW} = 10^{12}\,{\rm M}_\odot$), reconstructed via a Monte Carlo algorithm based on the Extended Press–Schechter formalizm (see Salvadori et al. 2007; de Bennassuti et al. 2014, for more details). Newly collapsed haloes are assumed to have a gas-to-dark matter mass ratio equal to the baryonic cosmic fraction, $M_g/M = \Omega_{\rm b}/\Omega_{\rm M}$ and a chemical composition equal to the Milky Way environment at their formation epoch. Hence they are all primordial, $Z = 0$, before the onset of SNe explosions. The main and new features of the model are summarized below, including the underlying key assumptions relevant for this work. We refer the reader to previous papers for more details.

Star formation. The SF is traced along the merger trees by adopting physically motivated hypotheses.

(i) There exists a minimum halo mass to form stars, $M_{sf}(z)$, whose evolution accounts for the suppression of SF in progressively *more massive* objects due to the increasing photodissociating and photoionizing radiation (Salvadori & Ferrara 2009, 2012). When the Milky Way environment is fully reionized, $z_{\rm rei} \approx 6$ (Salvadori et al. 2014), we assume that gas accretion is suppressed in haloes with virial temperatures $T_{\rm vir} \lesssim 2 \times 10^4$ K.

(ii) The SF rate, $\psi = \epsilon_* M_g/t_{\rm ff}$, which is regulated by the SF efficiency, ϵ_*, depends on the free-fall time, $t_{\rm ff}(z)$, and mass of cold gas in each galaxy, whose gradual accretion is described by a numerically calibrated infall rate (Salvadori, Ferrara & Schneider 2008).

(iii) In *minihaloes* with $T_{\rm vir} \lesssim 10^4$ K, the SF efficiency is assumed to be reduced as $\epsilon_{H_2} = 2\epsilon_*[1 + \left(T_{\rm vir}/2 \times 10^4 K\right)^{-3}]^{-1}$ to account for the ineffective cooling by molecular hydrogen, H_2 (Salvadori & Ferrara 2012).

(iv) Pop II stars with masses $m = [0.1 - 100]\,{\rm M}_\odot$ form according to a Larson initial mass function, $\Psi(m) = m^{-2.35} {\rm e}^{-0.35\,{\rm M}_\odot/m}$, if the gas metallicity exceeds the critical value, $Z_{\rm cr}$, which sets the minimal conditions for the formation of the first low-mass stars. This value can be either $Z_{\rm cr} = (10^{-4}$–$10^{-3})\,{\rm Z}_\odot$, if gas fragmentation is driven by metal-line cooling (e.g. Bromm et al. 2001; Frebel, Johnson & Bromm 2009), or $Z_{\rm cr} = (10^{-6}$–$10^{-4})\,{\rm Z}_\odot$, if it is due to thermal emission by collisionally excited dust grains (e.g. Schneider et al. 2002; Omukai et al. 2005). Following the most recent findings we set $Z_{\rm cr} = 10^{-4.15}\,{\rm Z}_\odot$ (e.g. Caffau et al. 2011; Schneider et al. 2012; de Bennassuti et al. 2014), and we explore the case $Z_{\rm cr} = 10^{-6}\,{\rm Z}_\odot$ in Section 6.

(v) Massive Pop III stars form if $Z < Z_{\rm cr}$. To work under the hypothesis that the early metal-enrichment is dominated by faint SN (e.g. Cooke & Madau 2014; de Bennassuti et al. 2014), we adopt the simplest prescription and assume that all Pop III stars have a characteristic stellar mass of $25\,{\rm M}_\odot$ and evolve as *faint SNe*, which experience mixing and fallback (e.g. Salvadori & Ferrara 2012).

Chemical enrichment. The contribution to the chemical enrichment by different stellar populations is traced in the code by accounting for the mass and metallicity dependent stellar lifetimes, and by including all chemical elements from C to Zn (Salvadori & Ferrara 2012). For Pop III stars evolving as faint SNe, we adopt the yields by Iwamoto et al. (2005) for the case.[2] Following Woosley & Weaver (1995), we assume that stars with $m > 40\,{\rm M}_\odot$ do not contribute to metal enrichment, and we adopt their yields systematically halved in iron (Timmes, Lauroesch & Truran 1995) for massive $8\,{\rm M}_\odot \leq m \leq 40\,{\rm M}_\odot$ stars that evolve as Type II SNe (SNeII), $\langle E_{\rm SNeII}\rangle = 1.2 \times 10^{51}$ erg. For low and intermediate mass AGB stars, $m < 8\,{\rm M}_\odot$, we adopt the yields by van den Hoek & Groenewegen (1997) for metallicities $Z > 10^{-3}$ and by Meynet & Maeder (2002) for $Z \leq 10^{-5}$. All relevant equations describing the chemical enrichment of star-forming galaxies can be found in Salvadori et al. (2008).

The contribution of Type Ia SNe (SNeIa) has been included by adopting the yields and explosion energy ($E_{\rm SNeIa} = 1.3 \times 10^{51}$ erg) by Iwamoto et al. (1999), and the bimodal delay time distribution observationally derived by Mannucci, Della Valle & Panagia (2006). At each time-step and for each star-forming halo of the merger tree we compute the rate of SNeIa by following Matteucci et al. (2006) and we fix the normalization constant, $A_{\rm SNeIa}$, to reproduce the actual rate of SNeIa in the Milky Way, $\approx (0.3/100)\,{\rm yr}^{-1}$ (Cappellaro, Evans & Turatto 1999).

The chemical evolution of the gas is simultaneously traced in the star-forming haloes and in the surrounding *Galactic medium*, or Milky Way environment, by including the effect of SN-driven outflows, which are regulated by the SN wind efficiency, ϵ_w. During SN explosions, metals present in the ISM are ejected out of the galaxy at a rate $\dot{M}_Z^{\rm ej} = Z\dot{M}_g^{\rm ej}$, where $Z = M_Z/M_g$ is the metallicity of the gas, and $\dot{M}_g^{\rm ej}$ the gas ejection rate, which depends on the cumulative SN explosion energy, and on the binding energy of the host halo (e.g. Salvadori et al. 2008; de Bennassuti et al. 2014). Heavy elements dispersed into the Milky Way environment are assumed to be instantaneously mixed in this medium, so its total metallicity, Z_{GM}, steadily increases across cosmic times.

Universality of the free parameters. The free parameters of the model are the SF and SN-wind efficiency (ϵ_*, ϵ_w), the critical metallicity ($Z_{\rm cr}$), and the fraction of stars that can give rise to SNeIa ($A_{\rm SNeIa}$). These are fixed to simultaneously reproduce the global properties of the Milky Way at $z = 0$, along with the MDF of Galactic halo stars (e.g. Salvadori et al. 2007; de Bennassuti et al. 2014). These free parameters are assumed to be *the same* for *all* the haloes of the merger tree and in *all* hierarchical merger histories of the Milky Way. Hence, the properties of different dwarf galaxies we will present in the following, are not the result of a fine tuning of the free parameters, but a consequence of the cosmological context in which we study the formation and evolution of these small systems.

Selection and properties of satellite candidates. Galaxies that can survive as satellites of the Milky Way are selected among star-forming haloes of the merger trees that at any given redshift have dark matter masses that correspond to low-sigma density fluctuations, $M < M_{2.5\sigma}(z)$. This assumption is supported by N-body simulations (e.g. Diemand, Madau & Moore 2005). After selection, its subsequent evolution is followed in isolation down to $z = 0$ (Salvadori & Ferrara 2009).

In Fig. 2, we show the predicted Fe–Luminosity relation for all selected candidates in 50 assembly histories of the Milky Way. We

[2] The total amount of Fe and C per stellar mass formed is equivalent to the integrated contribution of faint SN with $m = (10$–$40)\,{\rm M}_\odot$, as their yields are rescaled with stellar masses (e.g. fig. 2 by de Bennassuti et al. 2014) $25\,{\rm M}_\odot$ and kinetic explosion energy $E_{\rm PopIII} = 0.7 \times 10^{51}$ erg.

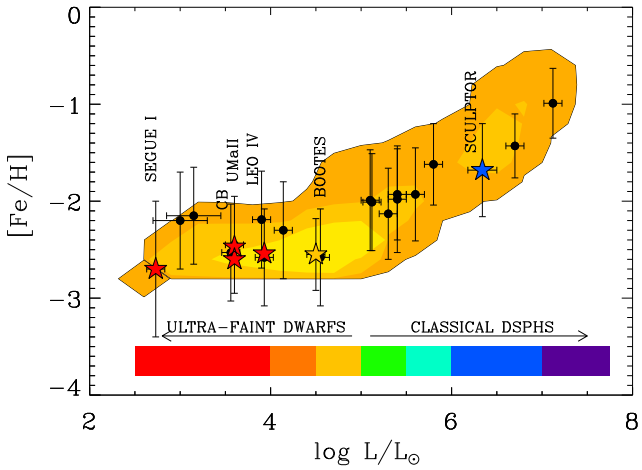

Figure 2. Predicted (contours) and observed (points) Fe–L relation for Milky Way dwarf galaxies. Contours identify regions containing the (68,95,99) per cent of the dwarf galaxy candidates in 50 hierarchical merger histories. Observed points are from Kirby et al. (2011). Stars and labels underline individual dwarf galaxies.

assume $M/L = 1$ to convert the stellar mass into total stellar luminosity, $L_* = M_* \times (L/M)$, and compare results with observations. We can see that model results match very well the observational data, including the nearly flat $\langle$[Fe/H]$\rangle$ value that is observed in ultra-faint dwarf galaxies. In Fig. 2, the coloured boxes identify galaxies in different luminosity ranges, using the same colour-code as in Fig. 1. These same colours will be used through the entire paper to distinguish among dwarf galaxies with different luminosities.

In our model, ultra-faint dwarf galaxies are predicted to be H_2-cooling minihaloes that form at $z > 7.5$, before photodissociation has suppressed gas cooling and SF in these small systems (Salvadori & Ferrara 2012). In contrast, classical dSph galaxies are predicted to form at later times through the merging of smaller progenitors. On average we find that the more luminous is a galaxy, the more massive is predicted to be its host halo, and the lower its final assembly redshift (Salvadori & Ferrara 2009). More luminous galaxies, therefore, keep accreting gas from the Galactic medium while it is increasingly polluted with the heavy elements ejected by low-mass star-forming galaxies.

We finally underline that in our model we do not account for mass transfer from binary companions. Thus, we can only investigate the incidence of CEMP(-no) stars that formed in carbon-enhanced environments.

4 RESULTS: THE GLOBAL PICTURE

We start by discussing the predictions of our cosmological model for the mean properties of dwarf galaxies in different luminosity ranges, which have been selected among all candidates in 50 different Milky Way realizations (Fig. 2). The main results are summarized in Fig. 3 where we show, for dwarf galaxies with increasing luminosities (from top to bottom), predictions for the average: (i) fraction of CEMP stars $F_{\rm CEMP}$ (left), (ii) normalized MDFs (middle), and (iii) low-Fe tails of the MDFs (right). The fraction of CEMP stars with respect to the total, $F_{\rm CEMP} = {N_{\rm L}}^{-1} \sum_{i=1}^{N_{\rm L}} N_*^{\rm CEMP}({\tt [Fe/H]})_i / N_*({\tt [Fe/H]})_i$, is calculated by averaging among the total number of dwarf galaxies within a given luminosity range, N_L, where $N_*^{\rm CEMP}({\tt [Fe/H]})_i$ is the fraction of CEMP stars in the ith galaxy, with a given [Fe/H] value. Similarly, we computed the mean MDFs by averaging among all $N_{\rm L}$ dwarf galaxies in a given L range. For reference, Segue 1, Coma Berenice, and Ursa Major II have luminosities consistent with galaxies in the top panel (red), Bootes in the third (yellow), and Sculptor in the second from bottom (blue).

Several interesting features can be noted in Fig. 3: (i) independent of galaxy luminosity, we find that $F_{\rm CEMP} = 1$ at [Fe/H] ≤ -5, and it rapidly decreases towards higher [Fe/H], with a steeper decline in more luminous dwarf galaxies. (ii) The shape of the normalized MDF dramatically changes with galaxy luminosity. In the least massive ultra-faint dwarf galaxies it is flat and covers a broad [Fe/H] range. As we move towards bigger galaxies, the MDF becomes more peaked, the peak is gradually shifted towards higher [Fe/H] values, and the low-Fe tail turns into a smaller fraction of the total. (iii) Stars with [Fe/H] < -3 are predicted to be found in *all* dwarf galaxies, but their relative contribution to the overall stellar populations strongly decreases when the luminosity of the galaxy increases, as shown by labels in the panels. (iv) On average, the cumulative number of stars at [Fe/H] < -4 is roughly of the same order of magnitude, $\approx$(1–2) $\times\ 10^3\ {\rm M}_\odot$, in all dwarf galaxies with the only exception of the faintest companions.

All these features are simply a result of the hierarchical galaxy formation process and the gradual *metal-enrichment* and *reionization* of the environment out of which these galaxies form, which imprint their physical properties. In our scenario, the faintest dwarf galaxies are associated with H_2-cooling minihaloes, which virialize from the Milky Way environment at $7.5 < z < 12$, when $-5 \leq {\rm [Fe/H]}_{GM} \leq -3$. The chemical enrichment proceeds very smoothly in these small systems, which transform gas into stars very inefficiently (Section 3; see also Salvadori & Ferrara 2009; Vincenzo et al. 2014; Webster, Sutherland & Bland-Hawthorn 2014; Bland-Hawthorn, Sutherland & Webster 2015; Romano et al. 2015). Roughly a constant number of stars are formed at different evolutionary phases (or [Fe/H]), and the gas can reach high [Fe/H] before being either completely evacuated by the cumulative effect of SNe explosions, or photoheated by the increasing external ionizing radiation (Salvadori & Ferrara 2012). This determines the characteristic shape of their MDF that is predicted, and observed, to be flat and to extend over a broad range of [Fe/H].

More luminous galaxies from via the assembly of these basics building blocks and more massive progenitors, which form afterwards. In this bottom-up scenario all dwarf galaxies are expected to have, on average, some ultra-faint dwarfs among their parent haloes. Hence, they are predicted to share similar number of stars and MDF tails at the lowest [Fe/H]. However, the more luminous a galaxy, the less prominent is the contribution of the few thousand stars formed in these lowest mass minihaloes into the final MDF. This is emphasized by the numbers reported in the right-hand panels of Fig. 3. We can see that extremely metal-poor stars represent $\geq$50 per cent of the stellar population in ultra-faint dwarfs, while they are only $\approx$0.3 per cent in dSph galaxies that have luminosity similar to Sculptor or higher. For this reason, the low-Fe tails seem to gradually 'disappear' in the normalized MDFs as the luminosity of the galaxies increases.

Since more massive dwarf galaxies complete their assembly at lower redshifts, they can continue accreting gas from a Milky Way environment that is increasingly polluted by heavy elements. The average ${\rm [Fe/H]}_{GM}$ value at the formation epoch of the main halo, where the bulk of the stars form, sets the lower limit of [Fe/H] in the normalized MDF. Thus, on average, the more luminous a galaxy, the more pronounced is the shift of its MDF towards higher [Fe/H]. Furthermore, galaxies hosted by more massive dark matter haloes have bigger gas reservoir, and they can more efficiently convert gas

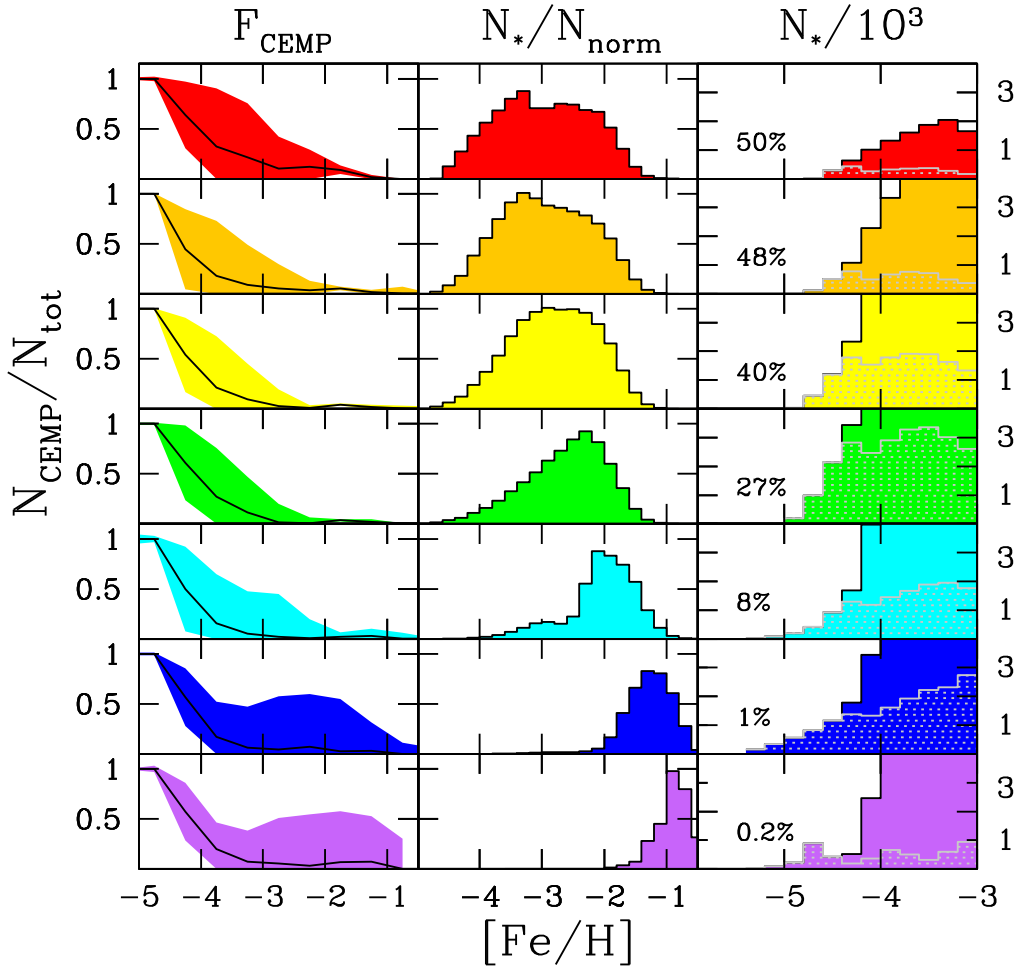

Figure 3. Average properties of stars at different [Fe/H] in Milky Way dwarf galaxies with increasing luminosity (from top to bottom): $L < 10^4\,L_\odot$ (red), $10^4\,L_\odot < L < 10^{4.5}\,L_\odot$ (orange), $10^{4.5}\,L_\odot < L < 10^5\,L_\odot$ (yellow), $10^5\,L_\odot < L < 10^{5.5}\,L_\odot$ (green), $10^{5.5}\,L_\odot < L < 10^6\,L_\odot$ (cyan), $10^6\,L_\odot < L < 10^7\,L_\odot$ (blue), $10^7\,L_\odot < L < 10^8\,L_\odot$ (bottom, violet). Left-hand panels: average fraction of CEMP stars (solid line) with $\pm 1\sigma$ dispersion (shaded area). Middle panels: average MDF normalized to the total number of stars (histogram). Right-hand panels: MDFs for stars at [Fe/H] < -3, showing both the total number of stars (filled histograms) and the number of CEMP-no stars (shaded grey histograms). The percentage shown is that of stars at [Fe/H] < -3 with respect to the total.

into stars because of their higher $T_{\rm vir} > 10^4$ K, which make them Ly α cooling haloes (e.g. Maio et al. 2007). This causes a gradually more pronounced peak in their MDFs.

The fraction of CEMP stars in dwarf galaxies with different luminosities is connected to all these previously presented effects. Looking at the right-hand panels of Fig. 3, we can see that $N_{\rm CEMP}$ follows N_* at [Fe/H] < -4.5, in all dwarf galaxies. These CEMP-no stars are predicted to form in (progenitor) H_2-cooling minihaloes that have been predominantly polluted by primordial faint SNe. Because of the small amount of iron ($Y_{\rm Fe} \approx 4 \times 10^{-7}$), and the huge amount of carbon ($Y_{\rm C} \approx 10^{-2}$) produced by faint SNe, long-lived Pop II stars can already start to form in these small systems[3] when the ISM is self-enriched up to $[{\rm Fe/H}]_{\rm cr} \approx -8$, which corresponds to [C/Fe] $\approx +4$, and $Z \approx Z_{\rm cr} = 10^{-4.15}\,{\rm Z}_\odot$. After the formation of Pop II stars, normal SNeII rapidly start to contribute to the chemical enrichment of both the ISM, gradually decreasing the [C/Fe] level while [Fe/H] rises, and the Milky Way environment, increasing Z_{GM} up to $Z_{\rm cr}$. In analogy to what is found in the Galactic halo (Caffau et al. 2011; Placco et al. 2014), we predict that carbon-normal stars can start to form when [Fe/H] $\gtrsim -4.7$, which corresponds to $Z_{GM} > Z_{\rm cr}$, and therefore to the disappearance of Pop III stars (de Bennassuti et al. 2014).

Thus, we predict that $F_{\rm CEMP} = 1$ at [Fe/H] $\lesssim -4.7$ in all dwarf galaxies, and that this fraction rapidly decreases with increasing [Fe/H], because of the larger contribution of SNeII in both self-enriched and newly formed galaxies. CEMP-no stars populating the MDF at $-4 <$ [Fe/H] < -2, predominantly form in environment polluted by primordial faint SN and SNeII. Thus, they are all predicted to form in the very early stages of galaxy evolution. Interestingly, we can see that these CEMP-no stars efficiently form in dwarf galaxies like Bootes (yellow) and Draco (green), which are in the 'transition region' between ultra-faint dwarfs and classical dSph galaxies (Fig. 2). This is because these galaxies are associated with the most massive among minihaloes, with $T_{\rm vir} \approx 10^4$ K, which host Pop III stars as their least luminous companion, but have higher SF efficiencies (Section 3). More massive, classical dSph galaxies, have higher probabilities to have among their progenitor haloes Pop II galaxies that virialized from an environment pre-enriched up to

[3] Where the 'critical' iron-abundance is settled by the yields of faint SNe: $[{\rm Fe/H}]_{\rm cr} = \log(Z_{\rm cr}/{\rm Z}_\odot) - \log(Y_{\rm Z}/Y_{\rm Fe}) + \log(M_{\rm Z}/M_{\rm Fe})_\odot$.

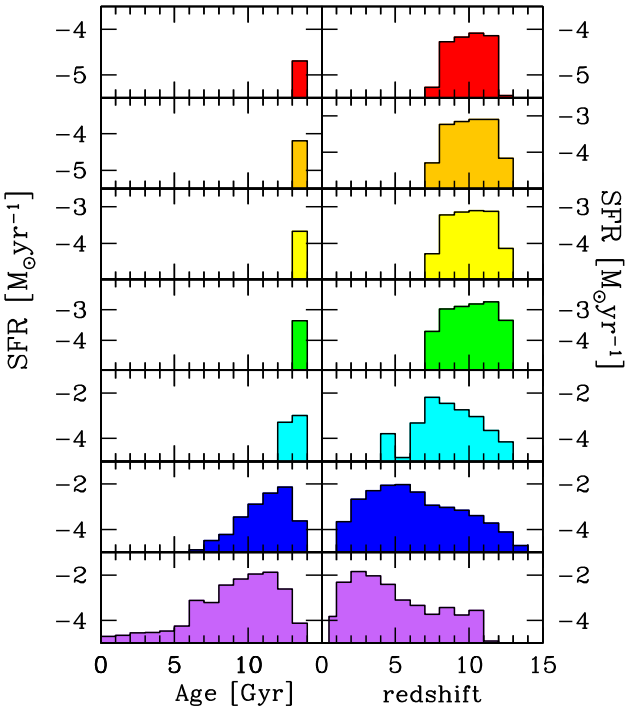

Figure 4. Predicted SF rates of Milky Way dwarf galaxies in different luminosity ranges (colours as described in Fig. 3) as a function of stellar ages (left) and redshift (right).

$[Fe/H]_{GM} \geq -4$ by normal SNeII (Salvadori et al. 2007; de Bennassuti et al. 2014). Carbon-normal stars efficiently form in these galaxies, causing the steeper decline of F_{CEMP} with [Fe/H].

In stars with higher iron-abundance, [Fe/H] > -2, we find that the carbon-enhancement might also come from low-metallicity ($Z \leq 10^{-3}$ Z$_\odot$) AGB stars, which evolve on longer time-scales. This causes the small increase of the F_{CEMP} values at [Fe/H] ≈ -1.5, which is visible in the left-hand panels of Fig. 3. Note that in our model we do not account for binary systems, so the carbon in these stars is not accreted from a companion, but it reflects the chemical composition of the birth environment. The products of AGB stars can be efficiently retained in the ISM of low-mass galaxies after SNeII have contributed to the chemical enrichment, and the galaxy can quietly evolve for a short period of time (e.g. Salvadori & Ferrara 2012). The production of s-process elements from $Z \leq 10^{-3}$ Z$_\odot$ AGB stars is still unclear (e.g. Fishlock et al. 2014) and we do not account for it in our work. However, these stars are most likely expected to be CEMP-s stars, although their properties are probably different from those formed in binary systems, which directly accrete material from an AGB companion.

Finally, we should emphasize that, although F_{CEMP} is steeper in more massive dwarfs, at [Fe/H] < -3 the results are all consistent within $\pm 1\sigma$ errors. As already discussed, this is because these different dwarf galaxies are expected to share similar ancestors at high redshift, namely low-mass H_2-cooling minihaloes, which represent the birth environments of stars at [Fe/H] < -3.

4.1 Star formation histories

Another way to consider these findings is to look at the predicted average SFHs of dwarf galaxies, which are shown in Fig. 4 as a function of stellar ages, and formation redshift. We can see that all dwarf galaxies are predicted to host stars >10 Gyr old, which is what is observed in the Local Group (e.g. Tolstoy, Hill & Tosi 2009). At very high redshifts, $z \geq 10$, we predict dwarf galaxies to share similar SF rates, $\psi \approx 10^{-3}$–10^{-4} M$_\odot$ yr^{-1}, independent of their total luminosity. It is during these cosmic epochs that the low-[Fe/H] tails of the MDFs are built-up in the star-forming progenitor minihaloes.

Ultra-faint dwarf galaxies are predicted to stop forming stars prior the end of reionization, $z > 6$, because of heating by the external UV background that prevents gas cooling, and 'sterilizes' those systems that still have some leftover gas to fuel SF (Salvadori & Ferrara 2012). This is consistent with observations of SFH in ultra-faint dwarfs (e.g. Brown et al. 2014). Note that some of these 'sterilized' minihaloes are predicted to evolve in isolation and survive until $z \approx 2$, when they can be observed as very-metal-poor Damped Ly Alpha systems (Salvadori & Ferrara 2012). These systems might re-start forming stars at later times (e.g. Ricotti 2009; Faerman, Sternberg & McKee 2013) and explain observations of H I-rich dwarf galaxies that show recent episodes of SF (e.g. LeoT: Irwin et al. 2007; de Jong et al. 2008; Weisz et al. 2012).

More luminous galaxies continue to efficiently form stars to much later times, and hence have more extended and complex SFHs. In the right-hand panels of Fig. 4, we see that ψ is expected to gradually increase towards lower redshifts, reaching the maximum at the main assembling epoch of the host halo, and decreasing afterwards, when the galaxy is assumed to evolve in isolation. The SFH that has been measured in the Sculptor dSph galaxy (de Boer et al. 2012), is qualitatively consistent with the one that we predict for dwarf galaxies with similar luminosity (blue): it has a peak at ≈13 Gyr, and then declines with cosmic time, lacking stars <6 Gyr old.

In this global picture we can therefore explain the variation, with galaxy luminosity, of both the MDFs and SFHs of dwarf galaxies.

5 DATA COMPARISON

We now test the results of our cosmological model against available observations for CEMP stars in nearby dwarf galaxies. We focus on three classes of dwarf galaxies that reside in different luminosity ranges, as shown in Fig. 2: (i) the 'classical' dSph galaxy Sculptor, $L = 10^{6.3\pm0.2}$ L$_\odot$; (ii) the most luminous of the ultra-faint dwarf galaxies, Bootes, $L = 10^{4.5\pm0.2}$ L$_\odot$; and (iii) the least luminous ultra-faint dwarfs, $L < 10^4$ L$_\odot$: the combination of SegueI, Coma Berenice, Ursa Major II, and LeoIV. As pointed out in Section 2, the available data for Bootes are mostly blind to CEMP subclasses (s, r, and no). This represents a possible caveat for our comparison with CEMP-no models. Still, most of the CEMP stars found in this system have [Fe/H] < -3, which is the typical [Fe/H] range of CEMP-no stars (e.g. fig. 1 of Norris et al. 2013).

Given the low number of [C/Fe] measurements in dwarf galaxies (see Figs 5a, 6a,d), we computed the uncertainty of F_{CEMP} by using the results of Gehrels (1986) for Poisson statistics. We derived the 1σ upper (lower) confidence limits as $F^{up}_{CEMP} = 1.841/N_*([Fe/H])$ in case of non-detection ($F^{low}_{CEMP} = 0.0$), and as $F^{up}_{CEMP} = 3.300/N_*([Fe/H])$ for single detection ($F^{low}_{CEMP} = 0.173/N_*([Fe/H])$), where $N_*([Fe/H])$ represents the total number of stars with available carbon measurements in different [Fe/H] ranges. So the fewer the measurements, the larger the uncertainties.

We used a Monte Carlo technique to randomly select from the mean theoretical MDFs, a number of stars equal to the total number of [Fe/H] measurements in different dwarf galaxies, N_{tot}. We then constructed the average $\pm 1\sigma$ errors on the MDF by iterating this procedure 100 times. These errors, which are shown in Figs 5(b) and 6(b,e) together with the dispersion among different dwarf

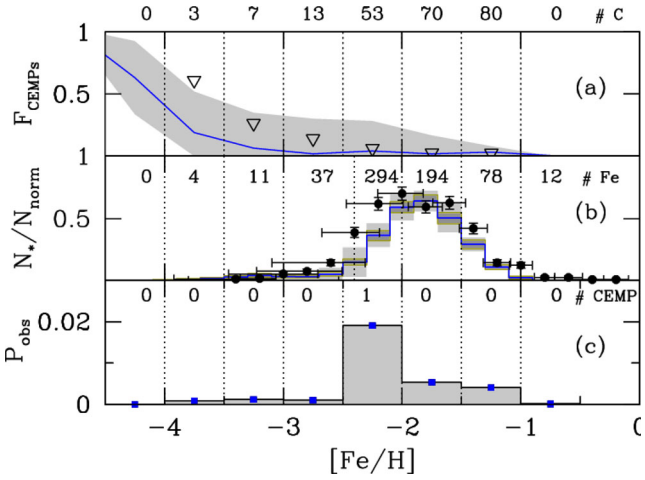

Figure 5. Predictions versus observations for the Sculptor dSph galaxy. Top panel: the fraction of CEMP stars in different [Fe/H] bins. The solid line shows the average value in the model, and the shaded area the $\pm1\sigma$ dispersion among different Sculptor-like dwarf galaxies (as Fig. 3). Upside down triangles are upper limits for the observed fraction of CEMP stars based on available data. Labels indicate the number of [C/Fe] measurements in each [Fe/H] bin (references in Fig. 1). Middle panel: the observed (points with error bars) and predicted MDF (histograms with shaded uncertainty). We show the $\pm1\sigma$ dispersion among Sculptor-like dwarf galaxies in 50 Milky Way possible assembling histories (light grey), and among 100 Monte Carlo sampling of the average MDF to the number of stars observed (dark grey). Labels indicate the number measurements in each [Fe/H] bin (Kirby et al. 2011; Starkenburg et al. 2013). Bottom panel: conditional probability to observe a star at a given [Fe/H] that it is also carbon-enhanced. Labels indicate the number of [C/Fe] > 0.7 measurements in each [Fe/H].

galaxies, provide an estimate of the data-driven uncertainties, i.e. they are the errors we always have to deal with while comparing theoretical models with small numbers of measurements.

5.1 Carbon-enhanced stars in Sculptor

The predicted average properties of Sculptor-like dwarf galaxies are shown in Fig. 5. We note that there is only one detection of a CEMP-no star in Sculptor at $-2.5 < [Fe/H] \leq -2$ (Skúladóttir et al. 2015), from which we get $F^{up}_{CEMP} = 0.06$. In the other [Fe/H] bins, with zero detections, F^{up}_{CEMP} is simply set by the number of [C/Fe] measurements. So the decline of F^{up}_{CEMP} towards higher [Fe/H] is simply a consequence of the larger number of stars observed at increasing [Fe/H].

From Fig. 5(a), we can see that the theoretical predictions are consistent with F^{up}_{CEMP}. As we already discussed in Section 4, because of the early chemical enrichment by primordial faint SN, F_{CEMP} rapidly declines with [Fe/H], ranging from unity at $[Fe/H] \leq -4.75$ down to values <0.005, at $[Fe/H] > -1$. Carbon-normal stars begin to form when $[Fe/H] \geq -4.7$, and in Sculptor they are predicted to be the majority of the stellar population (>50 per cent) already at $[Fe/H] \geq -4.25$. This result has two implications: (i) to catch second-generation stars imprinted *mainly* by primordial faint SNe in Sculptor, we should look among stars at $[Fe/H] < -4.75$, as in the Galactic halo; (ii) to increase the probability of finding CEMP stars in Sculptor we should follow up $[Fe/H] < -3$ stars, for which we predict $F_{CEMP} \geq 0.065$. Our ability to find these CEMP stars will remain naturally limited by the absolute number of stars that exist at these low [Fe/H]. Our model predicts, and this is supported by observations, that stars at $[Fe/H] < -3$ are *intrinsically* rare in luminous, Sculptor-like galaxies, only representing <3 per cent of the total stellar population (see Fig. 3). This point is highlighted in Fig. 5(b), where we compare the predicted and observed MDFs, that are normalized to the total number of stars. Noticeably, stars at $[Fe/H] < -3$ are almost invisible in the normalized function, which is dominated by more Fe-rich stars. Clearly, the paucity of stars at this low [Fe/H] makes it very challenging to search for CEMP-no stars in Sculptor, where only the brighter stars at the tip of the RGB can be followed up. Between $-3.5 \leq [Fe/H] < -3$, for example, we should roughly double the number of stars *found* in Sculptor to be able to observe one CEMP-no star among them.

Thus, we can ask a different question: What is the joint probability to observe a star that has a given [Fe/H] value, and that is also carbon-enhanced? Fig. 5(c) shows this joint probability distribution. This has been computed by combining the two independent functions: the fraction of CEMP stars *predicted* by the model, and the *observed* MDF normalized to the total number of stars, $P_{obs} = F_{CEMP} \times N_*/N_{tot}$. The probability, P_{obs}, is maximal at $[Fe/H] \approx -2$, where we predict the highest absolute number of CEMP stars. This result naturally explains why the first

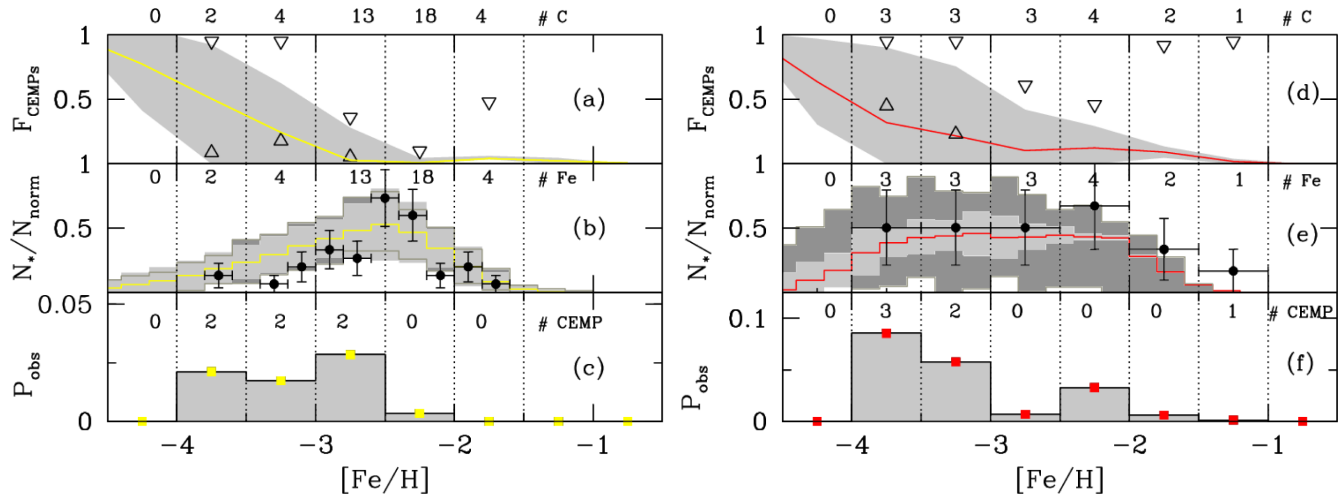

Figure 6. Same as Fig. 5 but for Bootes-like dwarf galaxies (left), and for the least luminous ultra-faint dwarfs with $L < 10^4\ L_\odot$ (right). Measurements are the same reported in Fig. 1. For F_{CEMP}, we show both upper and lower limits from observations (see text).

carbon-enhanced star in the Sculptor dSphs has been serendipitously found at such a high [Fe/H]. In conclusion, the observed MDF, the derived upper limits for $F_{\rm CEMP}$, and the iron-abundance of the only CEMP star detected in Sculptor, are all consistent with the hypothesis that faint SNe were the main contributors to primordial metal-enrichment.

5.2 Carbon-enhanced stars in ultra-faint dwarfs

We now explore the predictions of our model for less luminous ultra-faint dwarf galaxies, where many CEMP stars have been found (Fig. 1). In Fig. 6, we show the results for Bootes-like dwarf galaxies and for the least luminous ultra-faint dwarfs with $L < 10^4$ L$_\odot$. As for Sculptor we select these galaxies on the bases of their total luminosity among all the available candidates predicted by the model (Fig. 2).

By inspecting Figs 6(a) and (d), we can see that because of the low total number of stars observed in these small systems (≈40 in Bootes, and ≈15 in the faintest ultra-faint dwarf galaxies combined all together) the upper/lower limits on $F_{\rm CEMPs}$ are extremely high/low, and hence naturally consistent with model predictions. In these ancient systems, the fraction of RGB stars with respect to the total is estimated[4] to be $N_{\rm RGB}/N_*^{\rm tot} \approx 0.001$. This implies that in both cases ≥50 per cent of RGB stars have been already followed up.[5]

We note that in the model, the dispersion among different galaxies is huge in the case of the faintest dwarf galaxies (Fig. 6d), and at [Fe/H] = −3.5 the $+1\sigma$ error is consistent with $F_{\rm CEMP} \approx 0.8$. This is because these faint galaxies are associated with the least massive H_2-cooling minihaloes that are able to form stars, and which evolve in isolation. These systems can either virialize from a primordial birth environment, $Z < Z_{\rm cr}$, and hence $F_{\rm CEMP} \approx 1$ for [Fe/H] < −3 because they host primordial faint SN, or from a medium that has been pre-enriched up to $Z > Z_{\rm cr}$ by the products of SNeII. In the latter case they will only host Pop II stars, and hence $F_{\rm CEMP} \approx 0$. These different formation paths cause the large spread in $F_{\rm CEMP}$ at [Fe/H] < −3. According to our model, the large fraction of CEMP-no stars observed in the faintest dwarfs at [Fe/H] < −3 (≈80 per cent) suggests that these systems are *truly Pop III galaxies*, which have experienced primordial SF. However, we clearly need better measurement statistics. A quest for more data also emerges while comparing the predicted and observed MDFs (Fig. 6e). In the faintest dwarf galaxies, the errors induced by the low number of measurements (15 stars) are larger than the dispersion of the model among different dwarf galaxies and Milky Way merger histories. In contrast, these errors are equal (lower) than the intrinsic model uncertainties in Bootes (Sculptor), where ≈40 stars (≈700) have been observed.

Fig. 6(c and f) show the joint probability to observe a star in a given [Fe/H] range, that is also carbon-enhanced. If we compare this function with the one derived for Sculptor (Fig. 5c), we note a clear trend: the fainter the galaxy is, the higher is the *overall* probability to observe a star that is also carbon-enhanced, which is the integral of $P_{\rm obs}$ over the [Fe/H] range. This explains why it is much easier to find carbon-enhanced stars in these small systems. Moreover, $P_{\rm obs}$ is maximum at lower [Fe/H] in less luminous dwarf galaxies. For Bootes, we find that $P_{\rm obs}$ is maximum at $-4 \leq$ [Fe/H] ≤ -2.5, while for the faintest dwarfs at [Fe/H] ≤ −3. In both cases the predicted [Fe/H] ranges coincide with [Fe/H] values of observed CEMP-no stars in these small systems.

Finally, we should note that for the faintest dwarf galaxies the model predicts a non-negligible fraction of CEMP stars at [Fe/H] > −2 (upper panel). As explained in Section 4, these stars are predicted to form in environment polluted by the products of AGB stars with $Z < 10^{-3}$ Z$_\odot$, which can be retained by these small galaxies when SN have already exploded. Interestingly, a CEMP-s star at [Fe/H] ≈ −1.5 that does not show evidence for a binary companion has been recently detected in Segue 1 (Frebel et al. 2014). So, although more data are required to solidly assess if this star is in a binary system, this observation supports the idea that the physical mechanism we propose may contribute to the formation of CEMP-s in these small systems.

6 THE LOW-[FE/H] TAIL OF SCULPTOR

The results of our cosmological model show that CEMP-no stars, similar to those found in the Galactic halo and ultra-faint dwarfs, are not necessarily missing in classical dSph galaxies, such as Sculptor, but they could be *hidden* among rare [Fe/H] < −3 stars, which represent <3 per cent of the overall stellar population. The possible existence of a CEMP-no star at [Fe/H] = −3.77 (see Section 2) might be the first confirmation that this is indeed the case. Sculptor-like dSph galaxies, furthermore, are predicted to be among the best systems to find the most iron-poor stars, because their MDFs might extend down to [Fe/H] < −5, if faint SN dominated the early metal-enrichment (Fig. 3). The key question is: how much do we need to enlarge the current stellar sample to unveil the lowest Fe tail of the Sculptor MDF and catch the most pristine CEMP stars?

Fig. 7 shows how many stars at [Fe/H] < −3 are predicted to emerge in Sculptor-like dwarf galaxies by increasing the total number of [Fe/H] measurements. Fig. 7(a) exhibits results for the actual number of observed stars, ≈700 stars, which roughly correspond to ≈25 per cent of all RGB stars in Sculptor. Model predictions agree quite well with observations. Fig. 7(b) shows how the low-Fe tail of Sculptor will appear by following up all stars down to magnitudes $V \leq 20$, which corresponds to ≈1600 stars in the observed CMD (de Boer et al. 2012). We find that in this case we might be able to observe 12 ± 8 stars with [Fe/H] ≤ −4, the (40 ± 20) per cent of which are predicted to be CEMP-no stars. These observations can be achieved with present-day instrumentation [e.g. ESO Very Large Telescope (VLT) with X-Shooter, FLAMES, and UVES, or Keck/DIMOS] to add crucial information to our understanding of the properties of first stars and early galaxy formation processes. See for example Kirby et al. (2009), who used Keck/DIMOS to obtain medium-resolution spectra (6400–9000 Å, $R \approx 6500$) for $V \approx 20$ stars in the central region of Sculptor and derive their C and Fe abundances. Future generation of telescopes will allow us to measure [Fe/H] for stars below the main-sequence turn-off in nearby galaxies, like Sculptor. For example, the limit given for MOSAIC spectroscopy on the ESO-ELT (Evans et al. 2015) is $V \approx 25$ at $R \approx 15\,000$–$20\,000$. This will dramatically increase the number of stars that can be observed at high spectral resolution in nearby galaxies. The total number of RGB and MS stars in Sculptor with $V \leq 23$ is ≈20 000, and from these we can expect 80 ± 22 stars at [Fe/H] ≤ −4 (Fig. 7c), and 16 ± 10 stars with [Fe/H] ≤ −4.7, where the fraction of CEMP-no stars is expected to be 100 per cent. With these observations, furthermore, we might be able to accurately constrain the critical metallicity value. As already shown in Salvadori et al. (2007,

[4] We used PARSEC isochrones (Bressan et al. 2012; Chen et al. 2014; Tang et al. 2014), and the CMD generator available at http://stev.oapd.inaf.it/cmd.
[5] For the ultra-faint dwarfs this only is true if we consider the *combination* of the four systems at $L < 10^4$ L$_\odot$. In Segue I all RGB stars have already been followed up.

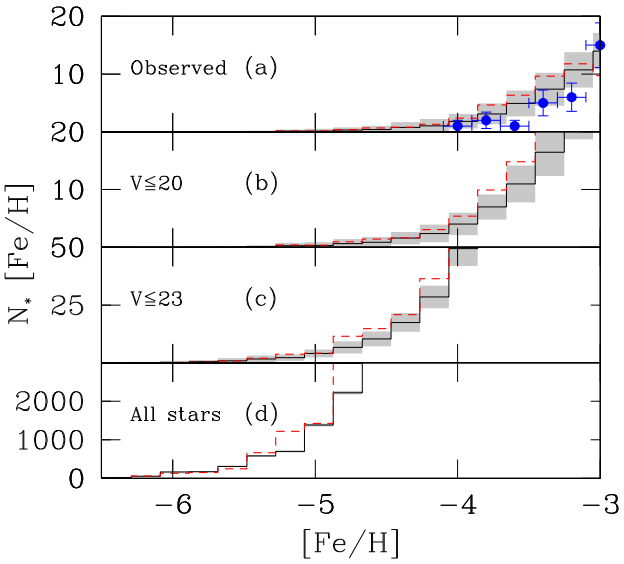

Figure 7. Number of stars at [Fe/H] < -3 that can be observed in Sculptor by increasing the sample of [Fe/H] measurements. From top to bottom we show results for: (i) the current statistics (≈700 RGB stars), where the available data are shown as points with Poissonian error bars (Fig. 5 for references); (ii) stars with $V \leq 20$; (iii) stars with $V \leq 23$; (iv) all stars. Shaded area show the $\pm 1\sigma$ errors obtained from the Monte Carlo random selection technique (see text). Solid histograms with shaded area are results for our fiducial model, $Z_{\rm cr} = 10^{-4.15}\,{\rm Z}_{\odot}$. Red dashed histograms show the same results for the case $Z_{\rm cr} = 10^{-6}\,{\rm Z}_{\odot}$.

fig. 7), decreasing $Z_{\rm cr}$ in the most feasible range, $Z_{\rm cr} \approx 10^{-4}$–$10^{-6}\,{\rm Z}_{\odot}$, mainly affects the number of long-lived stars at [Fe/H] < -4. Thus, the differences between $Z_{\rm cr}$ models become observable in Sculptor when a significant number of stars are followed up, and the lowest Fe tail starts to emerge (Fig. 7c,d).

7 SUMMARY AND DISCUSSION

We used a robust, data-constrained merger-tree model for the possible formation histories of the Milky Way and its dwarf satellites to predict the frequency of CEMP-no stars in nearby dwarf galaxies (e.g. Salvadori et al. 2008, 2014; Salvadori & Ferrara 2009, 2012). We have shown that the model can successfully explain the variation of the *average* MDFs and SFHs observed in dwarf galaxies with increasing luminosities (e.g. Kirby et al. 2011; Weisz et al. 2014) by accounting for SF in H_2-cooling minihaloes, $M = 10^{6.5}$–$10^{8}\,{\rm M}_{\odot}$, with a self-consistent treatment of the reionization and metal enrichment of the Milky Way environment.

By assuming that primordial faint SN, with mixing and fallback, dominated the early chemical enrichment, as suggested by observations of Galactic halo stars (e.g. Iwamoto et al. 2005; Cooke & Madau 2014; de Bennassuti et al. 2014; Marassi et al. 2014), we analyse the *average* properties of dwarf galaxies in different luminosity ranges, and show that:

(i) CEMP-no stars should exist in *all* dwarf galaxies within the observed luminosity range, $10^{2.5}\,{\rm L}_{\odot} < L < 10^{7.5}\,{\rm L}_{\odot}$.

(ii) Independent of galaxy luminosity the relative fraction of CEMP-no stars increases towards lower [Fe/H], reaching 100 per cent at [Fe/H] $\lesssim -4.7$.

(iii) As the galaxy luminosity increases, the overall probability to observe CEMP-no stars decreases, and the [Fe/H] range in which they are most likely to be found is shifted towards higher values.

(iv) In classical Sculptor-like dSph galaxies, the probability to find CEMP-no stars is almost an order of magnitude lower than in the faintest Milky Way companions, $L < 10^{4}\,{\rm L}_{\odot}$, and it is maximal, $P_{\rm obs} = 0.02$ at [Fe/H] ≈ -2.

The results explain why it is easier to discover CEMP-no stars in ultra-faint dwarf galaxies than in more luminous classical dSphs (e.g. Norris et al. 2010; Lai et al. 2011; Frebel et al. 2014), and also why the only CEMP-no star observed in Sculptor has been found at an unexpectedly high [Fe/H] (Skúladóttir et al. 2015). In particular, our model shows that CEMP-no stars at [Fe/H] $\lesssim -4.7$ form in environments predominantly polluted by primordial faint SN, which therefore have extremely high [C/Fe] values. On the other hand, those at $-4.7 \lesssim$ [Fe/H] $\lesssim -2.0$ are imprinted by both primordial faint SN and low metallicity, $Z < 10^{-3}\,{\rm Z}_{\odot}$, SNeII, in agreement with recent findings by Bonifacio et al. (2015). At [Fe/H] $\gtrsim -2.0$, we find that CEMP stars can also form in an ISM polluted by the products of AGB stars with $Z < 10^{-3}\,{\rm Z}_{\odot}$. Hence, they may potentially be enriched by s-process neutron capture elements (i.e. CEMP-s), which are not included in our model.

Our findings for CEMP-no stars, are a consequence of both the extremely low Fe-production, and high C, from faint SN, and of the cosmological context in which the hierarchical assembly of dwarf galaxies occurs. H_2-cooling minihaloes, or ultra-faint dwarf galaxies, $L < 10^{5}\,{\rm L}_{\odot}$, are thus predicted to be the high-redshift progenitors of more massive 'classical' dSph galaxies, and the environment of formation for stars with [Fe/H] < -3. The low-Fe tails of dwarf galaxies are thus expected to form in these common building blocks, some of which experienced Pop III SF (Salvadori et al. 2014). Such low-Fe tails can extend down to [Fe/H] < -4.7 if built-up upon the chemical products of primordial faint SN.

As the galaxy luminosity increases our model shows that the average MDFs become more *peaked*, and shifted towards *higher* [Fe/H] values, as is observed. Thus, stars at [Fe/H] < -3 become a *lower fraction* of the total stellar populations: from ≥40 per cent for ultra-faint dwarf galaxies, $L < 10^{5}\,{\rm L}_{\odot}$, to <0.2 per cent for $L > 10^{7}\,{\rm L}_{\odot}$. This is why in more massive dwarf galaxies the overall probability to observe a CEMP-no star decreases, and the [Fe/H] range in which they are more likely to be found increases. In Sculptor, $L \approx 10^{6.3}\,{\rm L}_{\odot}$, we find that the fraction of CEMP-no stars monotonically decreases from $F_{\rm CEMP} \approx 1$ at [Fe/H] ≤ -4.75 down to $F_{\rm CEMP} < 0.005$ at [Fe/H] ≥ -1. However, the probability to observe one of these stars is higher at $-2.5 <$ [Fe/H] ≤ -2 because more stars can be observed in this range.

A key prediction of our work is that galaxies with different luminosity are expected to share, on average, similar MDF tails *and* fractions of CEMP-no stars at the lowest [Fe/H]. At the moment, this hypotheses is supported by the observations of a very similar fraction of CEMP stars at [Fe/H] < -3 in the Galactic halo and in the *overall* sample of nearby dwarf galaxies, $F_{\rm CEMP}(\leq -3) \approx$ (43-42) per cent. However, more data need to be collected for the Milky Way companions. This also emerges from our analysis of the model uncertainties, which in the faintest dwarf galaxies are dominated by the low number statistics.

Finally, we should be clear that our model cannot exclude alternative scenarios for the formation of CEMP-no stars, such as metal pollution by massive rotating primordial stars (e.g. Meynet et al. 2006; Maeder et al. 2015). Furthermore, we did not explore the effects of different primordial initial mass functions on the fraction of CEMP-no stars in dwarf galaxies. Instead, we simply worked under the hypothesis that Pop III stars evolve as faint SN with mixing and fallback, since these pristine stars should dominate the

early chemical enrichment to successfully explain observations of CEMP-no stars in the Galactic halo (e.g. Cooke & Madau 2014; de Bennassuti et al. 2014). Our findings show that to further test the predominant role of primordial faint SN in the early Universe we need to at least double the current stellar sample in Sculptor, by measuring [Fe/H] and [C/Fe] in stars in different region of the galaxy down to magnitudes $V \leq 20$. Deeper observations ($V \leq 23$) should enable the discovery of peculiar CEMP-no stars in Sculptor similar to those found in the Galactic halo at [Fe/H] < -4. This will provide crucial information not only on the nature of first stars and critical metallicity value, but also on the formation of the Galactic halo, and hence on the underlying hierarchical galaxy formation process.

ACKNOWLEDGEMENTS

We thank the anonymous referee for his/her useful insights, and very constructive report. SS is grateful to P. Bonifacio and M. de Bennassuti for useful discussions. She warmly thanks J. Norris and E. Kirby for careful reading the first version of the paper, and C. Chiappini for key insights on early results. Finally, she is grateful to the Netherlands Organization for Scientific Research, which supports her research through a VENI grant 639.041.233.

REFERENCES

Abate C., Pols O. R., Karakas A. I., Izzard R. G., 2015, A&A, 576, A118
Allende Prieto C. et al., 2015, A&A, 579, A98
Aoki W., Beers T. C., Christlieb N., Norris J. E., Ryan S. G., Tsangarides S., 2007, ApJ, 655, 492
Asplund M., Grevesse N., Sauval A. J., Scott P., 2009, ARA&A, 47, 481
Beers T. C., Christlieb N., 2005, ARA&A, 43, 531
Benítez-Llambay A., Navarro J. F., Abadi M. G., Gottlöber S., Yepes G., Hoffman Y., Steinmetz M., 2015, MNRAS, 450, 4207
Bisterzo S., Gallino R., Straniero O., Cristallo S., Käppeler F., 2012, MNRAS, 422, 849
Bland-Hawthorn J., Sutherland R., Webster D., 2015, ApJ, 807, 154
Bonifacio P. et al., 2015, A&A, 579, A28
Bovill M. S., Ricotti M., 2009, ApJ, 693, 1859
Bovill M. S., Ricotti M., 2011, ApJ, 741, 18
Bressan A., Marigo P., Girardi L., Salasnich B., Dal Cero C., Rubele S., Nanni A., 2012, MNRAS, 427, 127
Bromm V., Ferrara A., Coppi P. S., Larson R. B., 2001, MNRAS, 328, 969
Brown T. M. et al., 2012, ApJ, 753, L21
Brown T. M. et al., 2014, ApJ, 796, 91
Caffau E. et al., 2011, Nature, 477, 67
Cappellaro E., Evans R., Turatto M., 1999, A&A, 351, 459
Chen Y., Girardi L., Bressan A., Marigo P., Barbieri M., Kong X., 2014, MNRAS, 444, 2525
Christlieb N. et al., 2002, Nature, 419, 904
Cohen J. G., Huang W., 2009, ApJ, 701, 1053
Cohen J. G., Christlieb N., Thompson I., McWilliam A., Shectman S., Reimers D., Wisotzki L., Kirby E., 2013, ApJ, 778, 56
Cooke R. J., Madau P., 2014, ApJ, 791, 116
Dall'Ora M. et al., 2012, ApJ, 752, 42
de Bennassuti M., Schneider R., Valiante R., Salvadori S., 2014, MNRAS, 445, 3039
de Boer T. J. L. et al., 2012, A&A, 539, A103
de Jong J. T. A. et al., 2008, ApJ, 680, 1112
Diemand J., Madau P., Moore B., 2005, MNRAS, 364, 367
Evans C. et al., 2015, preprint (arXiv:1501.04726)
Faerman Y., Sternberg A., McKee C. F., 2013, ApJ, 777, 119
Fishlock C. K., Karakas A. I., Lugaro M., Yong D., 2014, ApJ, 797, 44
Frebel A. et al., 2005, Nature, 434, 871
Frebel A., Johnson J. L., Bromm V., 2009, MNRAS, 392, L50
Frebel A., Kirby E. N., Simon J. D., 2010a, Nature, 464, 72
Frebel A., Simon J. D., Geha M., Willman B., 2010b, ApJ, 708, 560
Frebel A., Simon J. D., Kirby E. N., 2014, ApJ, 786, 74
Frebel A., Chiti A., Ji A. P., Jacobson H. R., Placco V. M., 2015, preprint (arXiv:1507.01973)
Gehrels N., 1986, ApJ, 303, 336
Gilmore G., Norris J. E., Monaco L., Yong D., Wyse R. F. G., Geisler D., 2013, ApJ, 763, 61
Hansen T., Andersen J., Nordtröm B., 2013, preprint (arXiv:1301.7208)
Hansen T. et al., 2015, ApJ, 807, 173
Hirano S., Hosokawa T., Yoshida N., Umeda H., Omukai K., Chiaki G., Yorke H. W., 2014, ApJ, 781, 60
Honda S., Aoki W., Arimoto N., Sadakane K., 2011, PASJ, 63, 523
Hosokawa T., Omukai K., Yoshida N., Yorke H. W., 2011, Science, 334, 1250
Irwin M. J. et al., 2007, ApJ, 656, L13
Iwamoto K., Brachwitz F., Nomoto K., Kishimoto N., Umeda H., Hix W. R., Thielemann F.-K., 1999, ApJS, 125, 439
Iwamoto N., Umeda H., Tominaga N., Nomoto K., Maeda K., 2005, Science, 309, 451
Jablonka P. et al., 2015, preprint (arXiv:1506.08636)
Joggerst C. C., Woosley S. E., Heger A., 2009, ApJ, 693, 1780
Keller S. C. et al., 2014, Nature, 506, 463
Kirby E. N., Guhathakurta P., Bolte M., Sneden C., Geha M. C., 2009, ApJ, 705, 328
Kirby E. N., Lanfranchi G. A., Simon J. D., Cohen J. G., Guhathakurta P., 2011, ApJ, 727, 78
Kirby E. N. et al., 2015, ApJ, 801, 125
Komiya Y., Suda T., Minaguchi H., Shigeyama T., Aoki W., Fujimoto M. Y., 2007, ApJ, 658, 367
Lai D. K., Lee Y. S., Bolte M., Lucatello S., Beers T. C., Johnson J. A., Sivarani T., Rockosi C. M., 2011, ApJ, 738, 51
Lee Y. S. et al., 2013, AJ, 146, 132
Lucatello S., Tsangarides S., Beers T. C., Carretta E., Gratton R. G., Ryan S. G., 2005, ApJ, 625, 825
McKee C. F., Tan J. C., 2008, ApJ, 681, 771
Madau P., Kuhlen M., Diemand J., Moore B., Zemp M., Potter D., Stadel J., 2008, ApJ, 689, L41
Maeder A., Meynet G., Chiappini C., 2015, A&A, 576, A56
Maio U., Dolag K., Ciardi B., Tornatore L., 2007, MNRAS, 379, 963
Mannucci F., Della Valle M., Panagia N., 2006, MNRAS, 370, 773
Marassi S., Chiaki G., Schneider R., Limongi M., Omukai K., Nozawa T., Chieffi A., Yoshida N., 2014, ApJ, 794, 100
Matteucci F., Panagia N., Pipino A., Mannucci F., Recchi S., Della Valle M., 2006, MNRAS, 372, 265
Meynet G., Maeder A., 2002, A&A, 390, 561
Meynet G., Ekström S., Maeder A., 2006, A&A, 447, 623
Meynet G., Hirschi R., Ekstrom S., Maeder A., Georgy C., Eggenberger P., Chiappini C., 2010, A&A, 521, A30
Muñoz J. A., Madau P., Loeb A., Diemand J., 2009, MNRAS, 400, 1593
Norris J. E., Christlieb N., Korn A. J., Eriksson K., Bessell M. S., Beers T. C., Wisotzki L., Reimers D., 2007, ApJ, 670, 774
Norris J. E., Gilmore G., Wyse R. F. G., Yong D., Frebel A., 2010, ApJ, 722, L104
Norris J. E. et al., 2013, ApJ, 762, 28
Okamoto S., Arimoto N., Yamada Y., Onodera M., 2012, ApJ, 744, 96
Omukai K., Tsuribe T., Schneider R., Ferrara A., 2005, ApJ, 626, 627
Pallottini A., Ferrara A., Gallerani S., Salvadori S., D'Odorico V., 2014, MNRAS, 440, 2498
Placco V. M., Frebel A., Beers T. C., Karakas A. I., Kennedy C. R., Rossi S., Christlieb N., Stancliffe R. J., 2013, ApJ, 770, 104
Placco V. M., Frebel A., Beers T. C., Stancliffe R. J., 2014, ApJ, 797, 21
Ricotti M., 2009, MNRAS, 392, L45
Romano D., Bellazzini M., Starkenburg E., Leaman R., 2015, MNRAS, 446, 4220
Salvadori S., Ferrara A., 2009, MNRAS, 395, L6
Salvadori S., Ferrara A., 2012, MNRAS, 421, L29
Salvadori S., Schneider R., Ferrara A., 2007, MNRAS, 381, 647

Salvadori S., Ferrara A., Schneider R., 2008, MNRAS, 386, 348
Salvadori S., Tolstoy E., Ferrara A., Zaroubi S., 2014, MNRAS, 437, L26
Schneider R., Ferrara A., Natarajan P., Omukai K., 2002, ApJ, 571, 30
Schneider R., Omukai K., Limongi M., Ferrara A., Salvaterra R., Chieffi A., Bianchi S., 2012, MNRAS, 423, L60
Shetrone M. D., Smith G. H., Stanford L. M., Siegel M. H., Bond H. E., 2013, AJ, 145, 123
Simon J. D., Frebel A., McWilliam A., Kirby E. N., Thompson I. B., 2010, ApJ, 716, 446
Simon J. D., Jacobson H. R., Frebel A., Thompson I. B., Adams J. J., Shectman S. A., 2015, ApJ, 802, 93
Skúladóttir Á., Tolstoy E., Salvadori S., Hill V., Pettini M., Shetrone M. D., Starkenburg E., 2015, A&A, 574, A129
Starkenburg E. et al., 2013, A&A, 549, A88
Starkenburg E., Shetrone M. D., McConnachie A. W., Venn K. A., 2014, MNRAS, 441, 1217
Suda T., Aikawa M., Machida M. N., Fujimoto M. Y., Iben I., Jr, 2004, ApJ, 611, 476
Tafelmeyer M. et al., 2010, A&A, 524, A58
Tang J., Bressan A., Rosenfield P., Slemer A., Marigo P., Girardi L., Bianchi L., 2014, MNRAS, 445, 4287
Timmes F. X., Lauroesch J. T., Truran J. W., 1995, ApJ, 451, 468
Tolstoy E., Hill V., Tosi M., 2009, ARA&A, 47, 371
Tominaga N., Iwamoto N., Nomoto K., 2014, ApJ, 785, 98
Umeda H., Nomoto K., 2003, Nature, 422, 871
van den Hoek L. B., Groenewegen M. A. T., 1997, A&AS, 123, 305
Venn K. A. et al., 2012, ApJ, 751, 102
Vincenzo F., Matteucci F., Vattakunnel S., Lanfranchi G. A., 2014, MNRAS, 441, 2815
Wang J., Frenk C. S., Navarro J. F., Gao L., Sawala T., 2012, MNRAS, 424, 2715
Webster D., Sutherland R., Bland-Hawthorn J., 2014, ApJ, 796, 11
Weisz D. R. et al., 2012, ApJ, 748, 88
Weisz D. R., Dolphin A. E., Skillman E. D., Holtzman J., Gilbert K. M., Dalcanton J. J., Williams B. F., 2014, ApJ, 789, 148
Woosley S. E., Weaver T. A., 1995, ApJS, 101, 181
Yong D. et al., 2013, ApJ, 762, 27

This paper has been typeset from a TEX/LATEX file prepared by the author.